

# Spatial Characteristics of the Difference between MISR and MODIS Aerosol Optical Depth Retrievals over Mainland Southeast Asia

Ningchuan Xiao,<sup>1</sup> Tao Shi,<sup>2</sup> Catherine A. Calder,<sup>2</sup> Darla K. Munroe<sup>1</sup>  
Candace Berrett,<sup>2</sup> Susan Wolfinbarger,<sup>1</sup> Dingmou Li<sup>1</sup>

<sup>1</sup> Department of Geography, The Ohio State University, Columbus, OH 43210

<sup>2</sup> Department of Statistics, The Ohio State University, Columbus, OH 43210

## Abstract

The difference between aerosol optical depths (AODs) retrieved from the Multi-angle Imaging SpectroRadiometer (MISR) and Moderate Resolution Imaging Spectroradiometer (MODIS) is examined over mainland Southeast Asia from a spatial perspective. Though ideally the differences between these measurement types should be small and randomly distributed over space, our analysis suggested that MISR/MODIS AOD differences have a strong negative relationship with MODIS AODs and tend to be spatially clustered. In this paper, we quantify the spatial dependence in MISR/MODIS AOD differences and explore the extent to which the spatial patterns in these differences can be explained by variables that reflect influence of the environment and human activities. While these variables show a significant relationship with MISR/MODIS AOD differences, the results also suggest further research is needed to fully understand the spatial dependence of these differences.

**Keywords:** Aerosol optical depth; MISR; MODIS; simultaneous autoregressive (SAR) model, spatial clustering; mainland Southeast Asia

## 1 Introduction

The Multi-angle Imaging SpectroRadiometer (MISR) and Moderate Resolution Imaging Spectroradiometer (MODIS) aboard the NASA Earth Observation System's Terra satellite are two major instruments designed to support aerosol optical depth (AOD) retrievals. While on the same satellite, aerosol products generated using data from these two sensors often exhibit noticeable differences. Though researchers have made insightful summaries of such differences (see, for example, Abdou et al., 2005; Kahn et al., 2005; Liu et al., 2007; Prasad and Singh, 2007; Jiang et al., 2007), the spatial characteristics of these AOD differences over a relatively large region have not been fully discussed (see a more detailed review in the next section). In studies using various aerosol data products, researchers typically expect the differences from multiple data sources to be relatively small and are randomly distributed across space and through time. This

assumption is often implicit in studies where multiple aerosol sources are used since only an overall correction (adjusting for the global difference) is made (Liu et al., 2007; Lyapustin et al., 2007). Here, we demonstrate that the difference between MISR/MODIS AODs are not in fact randomly distributed across space. We argue that better knowledge of the spatial characteristics of these differences is critical for environmental studies with a regional focus, where data over a large extent are needed but a global correction is insufficient and ground observations are only available for a limited number of locations. The difference between the two sensor retrievals may lead to different conclusions; systematic patterns of such differences in space may require further investigation and strategies for measurement adjustments may be needed.

The purpose of this paper is to illustrate the variation in the differences between MISR and MODIS AOD retrievals over the course of one year in an area with significant aerosol emissions, and myriad sources of aerosols including fossil fuel combustion for industrial activity and transportation, and biomass burning (Chin et al., 2002). More specifically, we are interested in exploring whether the differences exhibit significant patterns across space, by examining how much the difference between MISR and MODIS AODs varies locally, deviating from the regional (and perhaps global) overall pattern. We also examine whether the variation in these spatial differences correspond systematically to various factors that may influence the classification of aerosols and the underlying emissions processes, including land use, topography, and regional physical infrastructure. We focus our study on mainland Southeast Asia (roughly from 3°N 93°E to 25°N 109°E) where AODs may provide key and sensitive information to understanding the implications of biomass burning and increasing fossil fuel consumption.

In the remainder of this paper, Section 2 reviews the literature on comparison between MISR and MODIS AOD retrievals. In Section 3, we discuss a new pairing approach that is used to match MISR and MODIS AOD retrievals for our research region. Section 4 details the methods used in this research. The results are presented in Section 5. We finally conclude this paper in Section 6 with a discussion of the findings and future directions.

## **2 Background: comparing MISR and MODIS AOD retrievals**

Comparisons of MISR and MODIS AOD retrievals have been conducted in various locations for purposes such as city public health (Liu et al., 2007) and industrial pollution (Prasad and Singh, 2007). Many studies utilize ground AOD observations from the AERosol ROBotic NETwork (AERONET) as a means of validation (Chu et al., 2002; Abdou et al., 2005; Liu et al., 2007; Prasad and Singh, 2007; Kahn et al., 2007), while others focus on MISR and AERONET (Liu et al., 2004; Martonchik et al., 2004; Kahn et al., 2005; Jiang et al., 2007) or MODIS and MISR (Vermote et al., 2007) to understand the sensing capabilities of these instruments in a variety of contexts. Many issues arise in combining data from these three different sources, including consistency (Liu et al., 2007), combining data at different resolutions, as AERONET provides point data and MODIS and MISR area coverage, alignment issues (Abdou et al., 2005), as well as data availability issues including revisit times (Martonchik et al., 2004), sampling (Kahn et al., 2007), and data availability (Liu et al., 2007).

Researchers employed different spatial averaging techniques to deal with data assimilation challenges when they try to compare MISR, MODIS, and AERONET data. Liu et al. (2004) paired MISR pixels with AERONET locations that fall within the pixels; values from surrounding

pixels are averaged if the AERONET locations do not directly have MISR observations (Martonchik et al., 2004; Kahn et al., 2005; Jiang et al., 2007). To compare MISR and MODIS AODs, Abdou et al. (2005) averaged AOD values of up to 4 MODIS pixels in a  $\pm 0.5^\circ$  latitude and longitude box centered at a MISR pixel, while Liu et al. (2007) used the average AOD values in a  $3 \times 3$  MISR pixel window to match a  $5 \times 5$  window of MODIS pixels. Prasad and Singh (2007) used a nearest resampling approach to match Level 3 MISR and MODIS pixels with resolutions of  $0.5^\circ \times 0.5^\circ$  and  $1^\circ \times 1^\circ$ , respectively.

If multiple aerosol data products are to be used in integrated analyses, there must be best practice methods to employ these data in conjunction. MODIS and MISR aerosol measurements are expected to differ due to differing processing methods (Abdou et al., 2005), and algorithm and calibration differences (Kahn et al., 2007). In empirical comparisons, there have been a number of conflicting conclusions regarding the ways in which MODIS and MISR each record AOD, compared to each other and to the ground points provided by AERONET, respectively. Liu et al. (2007) conclude that MODIS and MISR can be used together, and a variety of other studies find the correlation sufficient to use the data in conjunction (Liu et al., 2004; Prasad and Singh, 2007; Jiang et al., 2007). When and where the sensors do not agree, studies have found discrepancies between retrievals under a variety of conditions. For example, MODIS and MISR both underestimate the AERONET measurements (Liu et al., 2007); MODIS retrieves higher values than MISR (Abdou et al., 2005; Liu et al., 2007) or that MISR overestimates (Liu et al., 2004) or underestimates (Jiang et al., 2007) AERONET values, depending on the specific context.

The discrepancies between MISR and MODIS correspond in part to location and physical geography. Abdou et al. (2005) and Kahn et al. (2005) identified key differences in retrievals over land versus water. Seasonal effects on retrievals are also prevalent (Liu et al., 2007; Kahn et al., 2005; Prasad and Singh, 2007; Jiang et al., 2007); MISR data are more accurate in the summer and winter (Prasad and Singh, 2007). Other factors that influence the difference are meteorological effects (Jiang et al., 2007), dust (Kahn et al., 2005; Martonchik et al., 2004) clear versus hazy days (Vermote et al., 2007), clouds (Martonchik et al., 2004; Kahn et al., 2007), anthropogenic influences (Prasad and Singh, 2007), the extent of biomass burning (Kahn et al., 2005), and sensitivity to differences in land and vegetation cover (Prasad and Singh, 2007).

Many researchers recognize the need to consider a regional scale of analysis, which may present challenges to current algorithms and data processing (Kahn et al., 2007), data integration (Liu et al., 2004), and data accuracy (Prasad and Singh, 2007). A detailed examination of the spatial characteristics of the difference between MISR and MODIS AODs over a large area (i.e., regional scale), however, has not yet been studied. As with many environmental processes, scale and extent of analysis has important implications for the utility, but also challenges, of integrated studies. In the remainder of this paper, we discuss this issue by focusing on the Southeast Asia mainland area where biomass burning is an important environmental concern to air quality and the use of MISR and MODIS AOD data is critical (Munroe et al., 2007).

### 3 Data

In this study, MISR AOD was obtained from the Earth Observing System Data Gateway. We used a Level 2 aerosol product called MISR\_AM1\_AS\_AEROSOL, where the data field RegBestEstimateSpectralOptDepth was extracted; versions F09\_0017 and F09\_0018 were used in

our study area. This data set has a spatial resolution of 17.6 km, and we used the blue (443 nm), green (555 nm), and red (670 nm) spectral bands in order to be comparable with MODIS bands. For MODIS AOD retrievals, we used a product called MOD04 where the data field Corrected\_Optical\_Depth\_Land was employed. This data field includes three spectral bands, blue (0.47  $\mu\text{m}$ ), green (0.55  $\mu\text{m}$ ), and red (0.66  $\mu\text{m}$ ). The spatial resolution for MOD04 is 10 km. Collection 005 of the MOD04 was used for our region.

An ideal situation for data comparison would include some ground observations. The spatial extent and temporal scheme of this research, however, limited the use of AERONET. In our study area, six AERONET stations are available, among which only three (Bac Giang, Mukdahan, and Pimai) have a significant number of observations in 2005. Unfortunately, none of the three stations have all of the days used in this research.

Two sampling strategies were used to create the data set for our study. To reduce temporal autocorrelation, we first extracted data for the first and fifteenth days of each month in 2005. Given the dates and spatial extent of our research, a total of 16 MISR paths (from path 123 to 138) were used. We then focused on MISR path 129 in our study area for the 22 days available in 2005 which would provide a more intensive view of the data. The total unique days used in this research was 44 (after considering the overlapping days in the two data sets).

To investigate the difference between MISR and MODIS AOD values, it is important to pair MISR and MODIS pixels so that the difference can be calculated. However, MISR and MODIS pixels do not exactly match each other because of their different scanning schemes. Figure 1A illustrates the locations of MISR and MODIS pixel centroids in part of our study area and Figure 1B shows the distribution of the distance between MISR pixels and their nearest MODIS pixels for our study area for all the data we acquired. In this research, instead of averaging the AOD data among several pixels which may lose some spatial information critical to this research, a new pairing approach was developed to preserve the basic spatial features of the original data and also to provide reasonable matching between MISR and MODIS AOD retrievals over a large region.

[Figure 1 here]

It can be observed from Figure 1A that MISR and MODIS pixels tend to overlap significantly, especially when they are close to each other. It is reasonable to pair a MISR pixel with a MODIS pixel if they are sufficiently close. We note that an objective threshold of such overlap may be difficult to determine. To create MISR/MODIS pixel pairs, we determined a distance threshold such that the overlapping area of the pixel pairs further apart than this distance will be less than 50 percent. Directly calculating the relationship between the overlapping area and MISR-MODIS pixel distance may be complicated due to the different scanning schemes of the two sensors (Figure 1A). Here we approximated this relationship by assuming that both MISR and MODIS pixels were squares and computing their overlap with respect to the distance between their centers and the relative position measured by the angle of the line formed by the two centers. Figure 1C illustrates a case where the distance is approximately 14 km and the angle is 35 degrees; the shaded shape represents the overlapping area which is about 10 percent of the area of a MISR pixel. The overall results are shown in Figure 1D. When the distance is set to 9 km, a majority of the relative positions between the approximate MISR and MODIS pixels will yield an overlap that is higher than 50 percent. Based on this analysis, we only considered the pairs of

MISR and MODIS pixels that were closer than or equal to 9 km. For all the dates in our study, there were a total of 13,890 pairs in which 12,268 pairs were within 9 km.

## 4 Methods

In general, we use  $\tau^{\text{MISR}}$  and  $\tau^{\text{MOD}}$  to denote the paired MISR and MODIS AOD values, respectively, and  $\delta$  to denote the difference between them. Specifically, the methods and results use the following notation.

$T$  = total number of days,  
 $N_t$  = total number of MISR/MODIS pixel pairs available for the  $t$ -th day,  
 $\tau_{it}^{\text{MISR}}$  = MISR AOD value for the  $i$ -th pixel pair on the  $t$ -th day,  
 $\tau_{it}^{\text{MOD}}$  = MODIS AOD value for the  $i$ -th pixel pair on the  $t$ -th day, and  
 $\delta_{it}$  = difference between the MISR and MODIS AOD values for the  $i$ -th pixel pair on the  $t$ -th day (i.e.,  $\delta_{it} = \tau_{it}^{\text{MISR}} - \tau_{it}^{\text{MOD}}$ )

### 4.1 Relationships between $\delta$ , $\tau^{\text{MISR}}$ , and $\tau^{\text{MOD}}$

We begin by exploring the relationship between  $\delta$ ,  $\tau^{\text{MISR}}$ , and  $\tau^{\text{MOD}}$  using the following simple linear regression models.

**Model A:**  $\tau_{it}^{\text{MISR}} = \alpha^A + \beta^A \tau_{it}^{\text{MOD}} + \epsilon_{it}^A$

**Model B:**  $\delta_{it} = \alpha^B + \beta^B \tau_{it}^{\text{MISR}} + \epsilon_{it}^B$

**Model C:**  $\delta_{it} = \alpha^C + \beta^C \tau_{it}^{\text{MOD}} + \epsilon_{it}^C$

where in each of the three models  $\alpha$  represents the intercept parameter,  $\beta$  is the regression coefficient parameter, and the  $\epsilon_{it}$ 's are independent and normally distributed random variables.

Model A can be used to quantify the strength of the linear relationship between the two AOD retrieval types; the values of  $\alpha^A$  and  $\beta^A$  being 0 and 1, respectively, indicates that an insignificant difference between MISR and MODIS AOD retrievals. Models B and C are designed to test the hypothesis that the difference between the two retrievals is not significantly dependent on either of the original retrievals (i.e., we expect  $\alpha^B$ ,  $\alpha^C$ ,  $\beta^B$ , and  $\beta^C$  to be close to 0).

### 4.2 Investigation of spatial variation of $\delta$

To analyze spatial patterns in the difference between paired MISR and MODIS AOD retrievals, we first define an  $N_t \times N_t$  binary spatial neighborhood matrix  $\mathbf{W}_t$  with the  $(i, j)$ -th element  $w_{ijt}$  equal to 1 if the centroids of the  $i$ -th and  $j$ -th pixel pairs on day  $t$  are within a specified distance (e.g., 100 km) of each other and 0 otherwise. With  $\mathbf{W}_t$  defined, we let matrix  $\tilde{\mathbf{W}}_t$  be the row-standardized version of  $\mathbf{W}_t$ , and its  $(i, j)$ -th element can be written as

$$\tilde{w}_{ijt} = \frac{w_{ijt}}{\sum_{j=1}^{N_t} w_{ijt}}.$$

We first examine the spatial pattern in the AOD differences using an exploratory approach based on the Moran's  $I$  statistics (see, for example, Cliff and Ord, 1981). For the  $t$ -th day, the Moran's  $I$  of the difference between MISR and MODIS AOD retrievals can be computed as

$$I_t = \frac{n \sum_{i=1}^{N_t} \sum_{j=1}^{N_t} \tilde{w}_{ijt} (\delta_{it} - \bar{\delta}_t) (\delta_{jt} - \bar{\delta}_t)}{\sum_{i=1}^{N_t} (\delta_{it} - \bar{\delta}_t)^2},$$

where  $\bar{\delta}_t = (1/N_t) \sum_{i=1}^{N_t} \delta_{it}$ . A positive  $I_t$  value indicates that on the  $t$ -th day there is positive spatial dependence in the difference between the MISR and MODIS AOD values, meaning similar values of AOD differences are clustered spatially; a negative  $I_t$  value means dissimilar values are clustered spatially. The further the value of  $I_t$  is from zero, the stronger the spatial dependence.

After using Moran's  $I$  statistics to explore the spatial dependence structure in the AOD differences, we employ a formal statistical model to examine whether the variation (both spatial and non-spatial) in the AOD differences can be explained by various covariates. We model  $\delta_{it}$  using a simultaneous autoregressive (SAR) error model (see, for example, Anselin, 1988). This model allows us to quantify the strength of the linear relationship between the observed AOD differences and a variety of covariate information while accounting for the residual spatial dependence structure in the differences. At time  $t$  ( $t = 1, \dots, T$ ) and location  $i$  ( $i = 1, \dots, N_t$ ) we assume that

$$\delta_{it} = \mathbf{X}_{it} \boldsymbol{\beta} + \phi_{it}$$

where  $\mathbf{X}_{it}$  is a  $1 \times P$  vector of  $P$  covariates associated with the  $i$ -th pixel pair on day  $t$ ,  $\boldsymbol{\beta}$  is a  $P \times 1$  vector of corresponding regression coefficients, and  $\phi_{it}$  is a spatially-dependent random error variable. Letting  $\boldsymbol{\phi}_t = [\phi_{1t}, \phi_{2t}, \dots, \phi_{N_t t}]'$ , we take

$$\boldsymbol{\phi}_t = \lambda \tilde{\mathbf{W}}_t \boldsymbol{\phi}_t + \boldsymbol{\epsilon}_t$$

where  $\lambda$  is an unknown spatial dependence parameter,  $\tilde{\mathbf{W}}_t$  is the known  $N_t \times N_t$  spatial neighborhood matrix defined above, and  $\boldsymbol{\epsilon}_t$  is a random error vector. We restrict  $\lambda \in [0, 1)$  to guarantee invertibility of the covariance matrix (for further details, see Banerjee et al., 2004). Finally, we assume that each  $\epsilon_{it} \sim N(0, \sigma^2)$ , and that they are independent for all  $i$  and  $t$ . The estimated values of  $\lambda$  can be interpreted analogously to the Moran's  $I$  statistics: the higher the value, the more spatially dependent the AOD differences after controlling for the covariate information.

## 5 Results

Using the pairing approach described in the data section above, the general relationship between MISR and MODIS AOD retrievals is summarized in the box plots in Figure 2 where the difference ( $\delta$ ) for all paired pixels are plotted. It can be observed that the mean  $\delta$  values are close to zero, with substantial variation around zero. It can also be noted from this figure that the difference among the three bands are relatively small.

[Figure 2 here]

We then map the difference between MISR and MODIS AOD retrievals over our study area (Figure 3). It can be observed that the difference exhibits spatial clustering for different paths and the same path. In Figure 3A, for example, spatial trends can be observed and the MISR/MODIS differences are often clustered with similar values. The same trend can also be observed in Figure 3B. Moreover, Figure 3B reveals another trend: MISR AOD retrievals tend to be lower than MODIS AOD values when the latter are high (the left map in Figure 3B), and vice versa.

[Figure 3 here]

## 5.1 Regional and local relationships between $\delta$ , $\tau^{\text{MISR}}$ , and $\tau^{\text{MOD}}$

We fit the three regression models using the data for all dates simultaneously and list the results in Table 1. All the estimated intercepts and coefficients in this table are significant at the 0.001 level. Though the  $r^2$  values for Model B are low, the estimates are still significant, mainly because of the large sample size (12,266 observations). Figure 4 summarizes the results from fitting the three models on all dates separately, which are generally consistent with the estimates described in Table 1. Based on this analysis, the following two observations can be made.

- From the results of Model A,  $\tau^{\text{MISR}}$  and  $\tau^{\text{MOD}}$  exhibit general agreement and show a strong positive linear relationship, as evidenced by the high  $r^2$  values. When all the days are considered together, a positive intercept ranging from 0.11 to 0.18 can be found for all bands (Table 1), and results are similar when days are used separately (the top plot in Figure 4).
- The difference between MISR and MODIS ( $\delta$ ) does not show a strong relationship with  $\tau^{\text{MISR}}$  values (Model B) as evidenced by the low  $r^2$  values (the middle plot in Figure 4). However, a strong negative linear relationship between  $\delta$  and  $\tau^{\text{MOD}}$  can be observed as the coefficient values for Model C are negative and the  $r^2$  values are relatively high (the bottom plot in Figure 4).

[Table 1 here]

[Figure 4 here]

## 5.2 Spatial clustering of $\delta$

Figure 5 shows the values of the Moran's  $I$  statistics for the AOD differences over the dates used in this research. Here, we tested three different neighborhood settings (i.e., the  $\mathbf{W}_t$  matrix) with distance thresholds of 50, 100, and 150 km, respectively. The results suggest a persistent positive clustering for most of the days. For a limited number of dates, the Moran's  $I$  values are smaller than zero (as the part of the plots that are below the horizontal line). According to the Moran's  $I$  hypothesis test for the degree of spatial dependence, however, all these negative statistics are

insignificant, while all other days have significant positive values. This finding supports the visual examination on the patterns in Figure 3, described at the beginning of this section.

[Figure 5 here]

To further analyze the strong spatial clustering feature of the difference between MISR and MODIS AOD retrievals, we applied the SAR model described in the previous section. We identified a set of covariates that have been considered to be important in terms of aerosol emission and dynamics (see, for example, Munroe et al., 2007). More specifically, we included two types of factors (Table 2). First, factors that reflect basic characteristics of the physical environment are considered, including the months of the dry season (from April to November) and elevation. Then, we identified a set of factors that are useful to account for the impact of human activities in this area, including seven land cover and land use types (water, forest, shrub, savanna, crop, wetland, and urban), and distance of each location to major roads (droads), coast (dcoast), cities with population greater 250,000 (dbcity), and other major cities (docity) with population less than 250,000. In addition to these two types of covariates, we included MODIS AOD retrievals because of its strong negative linear relationship with the MISR/MODIS AOD difference.

[Table 2 here]

Results from the SAR model are listed in Table 2. To provide a more detailed analysis, we specified two versions of the SAR model and fitted them using three different neighborhood definitions (again, the  $\mathbf{W}_t$  matrix) based on three distance thresholds (50, 100, and 150 km, respectively). The first version is a model that contains only two covariates ( $\tau^{\text{MOD}}$  and dry), while the second version is an extended model that includes all the covariates described above. The reason for the first model version to include a variable (dry) in addition to  $\tau^{\text{MOD}}$  is to account for possible monsoon effect that is pervasive and important in the study area. The second model does not include the intercept term in order to estimate effects corresponding to all land cover and land use types.

From Table 2, it can be observed that, except dcoast, dbcity, and docity, all other covariates can be concluded to be significantly related to the difference between MISR and MODIS AOD retrievals for all distance thresholds. This difference is significantly higher in the dry season, when biomass burning in the region is likely to occur. There are also meteorological differences in the dry season (e.g., high temperatures and low precipitation) that could contribute to the discrepancy in these two data products.

The relative difference between MISR and MODIS was on average highest over wetlands and savanna and lowest over forest and urban. The difference between MISR and MODIS increases with respect to elevation (though this coefficient is small), indicating that the difference is higher in more mountainous areas. This effect could also be capturing meteorological variation, or could result from the fact that biomass burning associated with shifting cultivation is more likely to happen in mountainous areas (Fox et al., 2000).

With regards to the influence of physical infrastructure, the difference decreased with distance from roads, or the difference in the two products is larger close to roads. This effect could be in part capturing the effect of air pollution due to automotive travel and other industrial

activity. There was no significant effect of proximity to other significant cities on the difference between MISR and MODIS.

Table 2 indicates that the regression findings are robust to the specification of the spatial weights matrix, except for the influence of distance to large cities, where the value goes from negative and significant, to positive and significant, to insignificant with the changes in the weights matrix.

In the SAR model, the  $\lambda$  value indicates residual spatial dependence. A high, significant  $\lambda$  value suggests that the current model exhibits a significant level of spatial dependence that cannot be fully accounted for by the covariates used. This is the case for all of our SAR modeling results (Table 2). By comparing the two versions of the models, it can be found that though introducing more covariates in an extended model can decrease spatial dependence, doing so does not make a significant impact in terms of reducing spatial dependence. This result is robust for all the three neighborhood settings tested.

## 6 Discussion and Conclusions

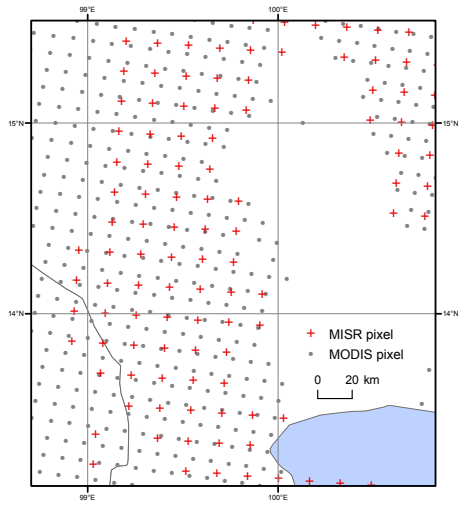
In this paper, we examine the relationship between MISR and MODIS AOD retrievals over mainland Southeast Asia from a spatial perspective. By pairing the nearest MISR and MODIS pixels, our results generally confirm the findings in the literature that both retrieval types are highly correlated. It has been discussed in the literature that MISR red and near-infrared bands are consistently too bright by 3 and 1 percent, respectively, relative to independent standards (see, for example, Bruegge et al., 2003; Abdou et al., 2005; Kahn et al., 2005). Our study shows that such a relationship exhibits a substantial variation which may need to be considered for many environment research and applications at a regional level.

We reported a spatial clustering pattern in the difference between MISR and MODIS AOD retrievals in our study area. This pattern is consistent across different neighborhood definitions. We note that MISR/MODIS AOD differences have a strong negative relationship with MODIS AOD retrievals. We examined a number of factors that are important to understanding the differences, but the results are not conclusive in terms of narrowing down all the influencing variables. As a direction of future research, it will be interesting to explore other factors that may provide a more insightful explanation to clustering patterns. Some recent studies may lead to fruitful future research in this area. For example, Kahn et al. (2007) discussed algorithm issues and suggested potential upgrades; Abdou et al. (2005) highlighted problems with calibration differences, aerosol model differences, and algorithm assumptions that will influence data analysis; Jiang et al. (2007) suggest that the aerosol models for MISR should be changed to better fit high-pollution areas; Liu et al. (2004, 2007) suggested more fine-scale satellites to gain more accurate data. Among many possible future directions, a detailed analysis of MISR and MODIS AOD retrieval algorithms will provide insightful information about the spatial pattern of their difference. Specifically, it will be interesting to examine how these algorithms deal with cloud screening and ground information and how such discrepancy affect their aerosol products.

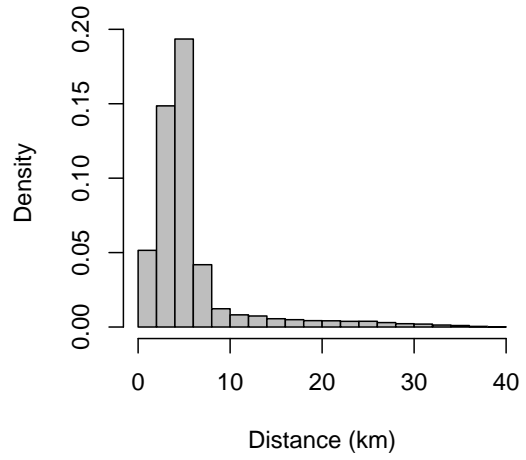
## References

- Abdou, W. A., D. J. Diner, J. V. Martonchik, C. J. Bruegge, R. A. Kahn, B. J. Gaitley, K. A. Crean, L. A. Remer, and B. Holben (2005). Comparison of coincident Multiangle Imaging Spectroradiometer and Moderate Resolution Imaging Spectroradiometer aerosol optical depths over land and ocean scenes containing Aerosol Robotic Network sites. *Journal of Geophysical Research* 110, D10S07, doi:10.1029/2004JD004693.
- Anselin, L. (1988). *Spatial Econometrics: Models and Methods*. Dordrecht: Kluwer Academic Publishers.
- Banerjee, S., B. P. Carlin, and A. E. Gelfand (2004). *Hierarchical Modeling and Analysis for Spatial Data*. Boca Raton: Chapman & Hall/CRC.
- Bruegge, C. J., W. Abdou, D. J. Diner, B. J. Gaitley, M. Helmlinger, R. A. Kahn, and J. V. Martonchik (2003). Validating the MISR radiometric scale for the ocean aerosol science communities. In *Proceedings of the International Workshop on Radiometric and Geometric Calibration*, pp. 103–115. Gulfport, Mississippi.
- Chin, M., P. Ginoux, S. Kinne, O. Torres, B. Holben, B. Duncan, R. Martin, J. Logan, A. Higurashi, and T. Nakajima (2002). Tropospheric aerosol optical thickness from GOCART model and comparisons with satellite and sun photometer measurement. *Journal of the Atmospheric Sciences* 59, 461–483.
- Chu, D. A., Y. J. Kaufman, C. Ichoku, L. A. Remer, D. Tanre, and B. N. Holben (2002). Validation of MODIS aerosol optical depth retrieval over land. *Geophysical Research Letters* 29(12), 10.1029/2001GL013205.
- Cliff, A. D. and J. K. Ord (1981). *Spatial processes: Models and Applications*. London: Pion.
- Fox, J., D. Truon, A. Rambo, N. Tuyen, L. Cuc, and S. Leisz (2000). Shifting cultivation: a new old paradigm for managing tropical forests. *Bioscience* 50(6), 521–528.
- Jiang, X., Y. Liu, B. Yu, and M. Jiang (2007). Comparison of MISR aerosol optical thickness with AERONET measurements in Beijing metropolitan area. *Remote Sensing of Environment* 107(1-2), 45–53.
- Kahn, R., W.-H. Li, J. V. Martonchik, C. J. Bruegge, D. J. Diner, B. J. Gaitley, W. Abdou, O. Dubovik, B. Holben, A. Smirnov, Z. Jin, and D. Clark (2005). MISR calibration, and implications for low-lightlevel aerosol retrieval over dark water. *Journal of the Atmospheric Sciences* 62(4), 1032–1052.
- Kahn, R. A., B. J. Gaitley, J. V. Martonchik, D. J. Diner, and K. A. Crean (2005). Multiangle Imaging Spectroradiometer (MISR) global aerosol optical depth validation based on 2 years of coincident Aerosol Robotic Network (AERONET) observations. *Journal of Geophysical Research* 110, D10S04, doi:10.1029/2004JD004706.

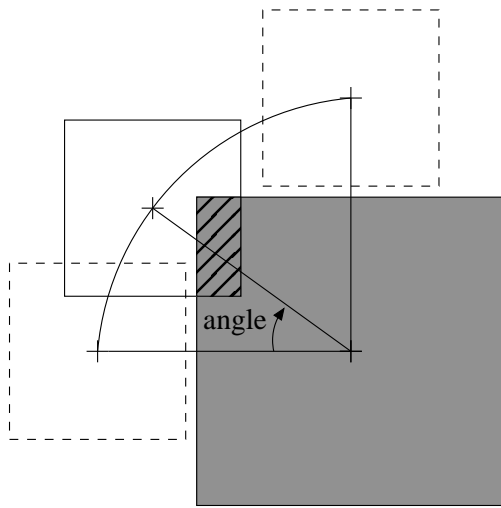
- Kahn, R. A., M. J. Garay, D. L. Nelson, K. K. Yau, M. A. Bull, B. J. Gaitley, J. V. Martonchik, and R. C. Levy (2007). Satellite-derived aerosol optical depth over dark water from MISR and MODIS: Comparisons with AERONET and implications for climatological studies. *Journal of Geophysical Research* 112, doi:10.1029/2006JD008175.
- Liu, Y., M. Franklin, R. Kahn, and P. Koutrakis (2007). Using aerosol optical thickness to predict ground-level PM<sub>2.5</sub> concentrations in the St. Louis area: A comparison between MISR and MODIS. *Remote Sensing of Environment* 107, 33–44.
- Liu, Y., J. A. Sarnat, B. A. Coull, P. Koutrakis, and D. J. Jacob (2004). Validation of Multiangle Imaging Spectroradiometer (MISR) aerosol optical thickness measurements using Aerosol Robotic Network (AERONET) observations over the contiguous United States. *Journal of Geophysical Research* 109, D06205, doi:10.1029/2003JD003981.
- Lyapustin, A., Y. Wang, R. Kahn, J. Xiong, A. Ignatov, R. Wolfe, A. Wu, B. Holben, and C. Bruegge (2007). Analysis of MODIS-MISR calibration differences using surface albedo around AERONET sites and cloud reflectance. *Remote Sensing of Environment* 107, 12–21.
- Martonchik, J. V., D. J. Diner, R. Kahn, B. Gaitley, and B. N. Holben (2004). Comparison of MISR and AERONET aerosol optical depths over desert sites. *Geophysical Research Letters* 31, L16102.
- Munroe, D. K., S. R. Wolfenbarger, C. A. Calder, T. Shi, N. Xiao, C. Q. Lam, and D. Li (2007). The relationships between biomass burning, land-cover/use change, and the distribution of carbonaceous aerosols in mainland Southeast Asia: A review and synthesis. Technical report no. 793, Department of Statistics, The Ohio State University.
- Prasad, A. K. and R. P. Singh (2007). Comparison of MISR-MODIS aerosol optical depth over the Indo-Gangetic basin during the winter and summer seasons (2000-2005). *Remote Sensing of Environment* 107(1-2), 109–119.
- Vermote, E. F., J. C. Roger, A. Sinyuk, N. Saleous, and O. Dubovik (2007). Fusion of MODIS-MISR aerosol inversion for estimation of aerosol absorption. *Remote Sensing of Environment* 107(1-2), 81–89.



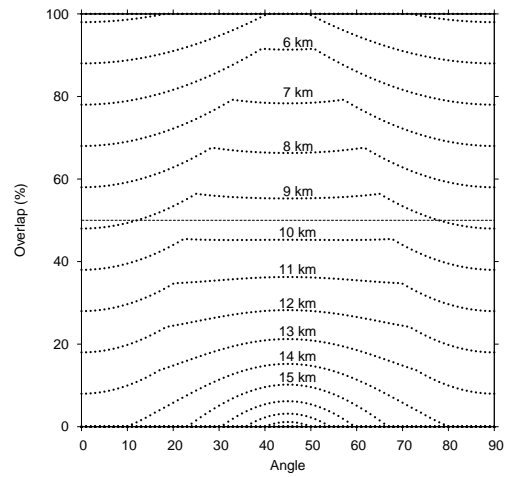
(A)



(B)



(C)



(D)

Figure 1: Pairing MISR and MODIS pixels. (A) The locations of MISR and MODIS pixel centroids in a part of our study area. (B) Distribution of the nearest distance between MISR and MODIS pixel centroids. (C) An approximation of calculating the overlap between a MISR pixel and MODIS pixel. (D) The relationship between MISR/MODIS pixel overlap with respect to their distance and relative position.

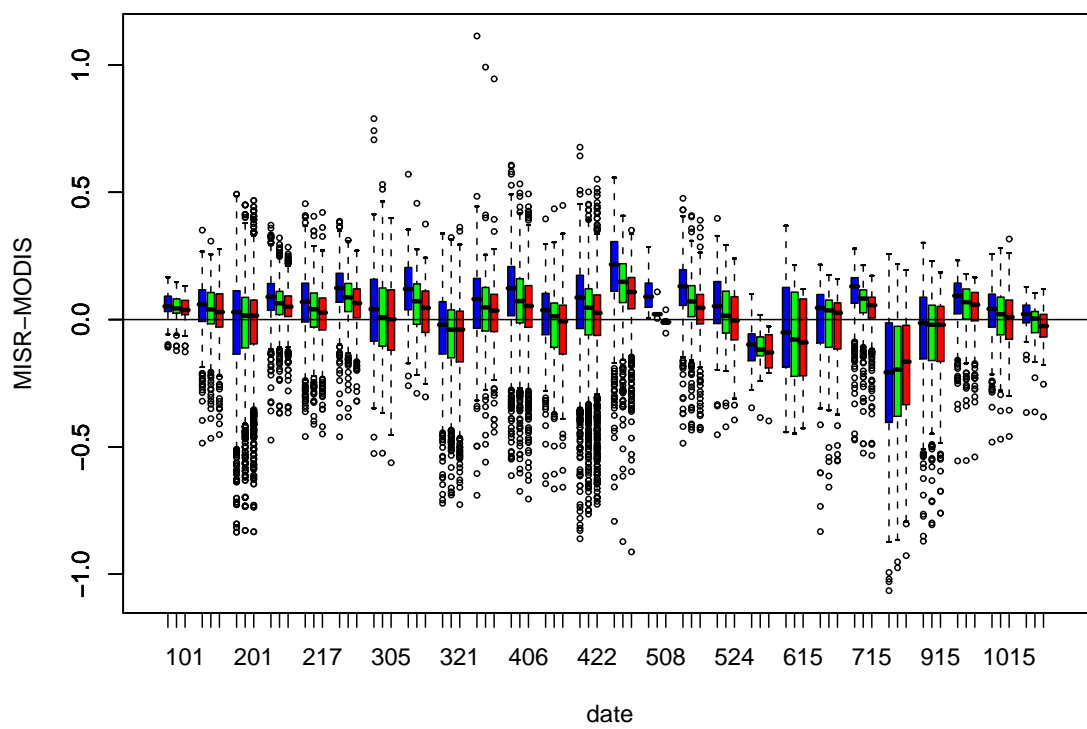
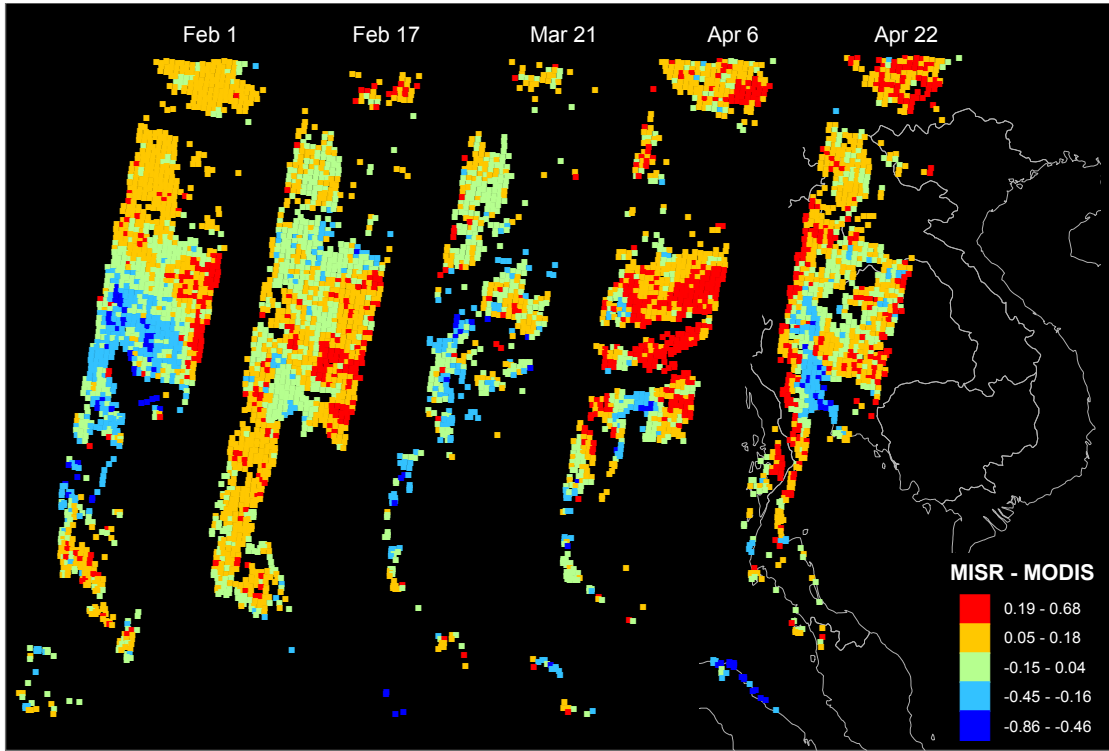
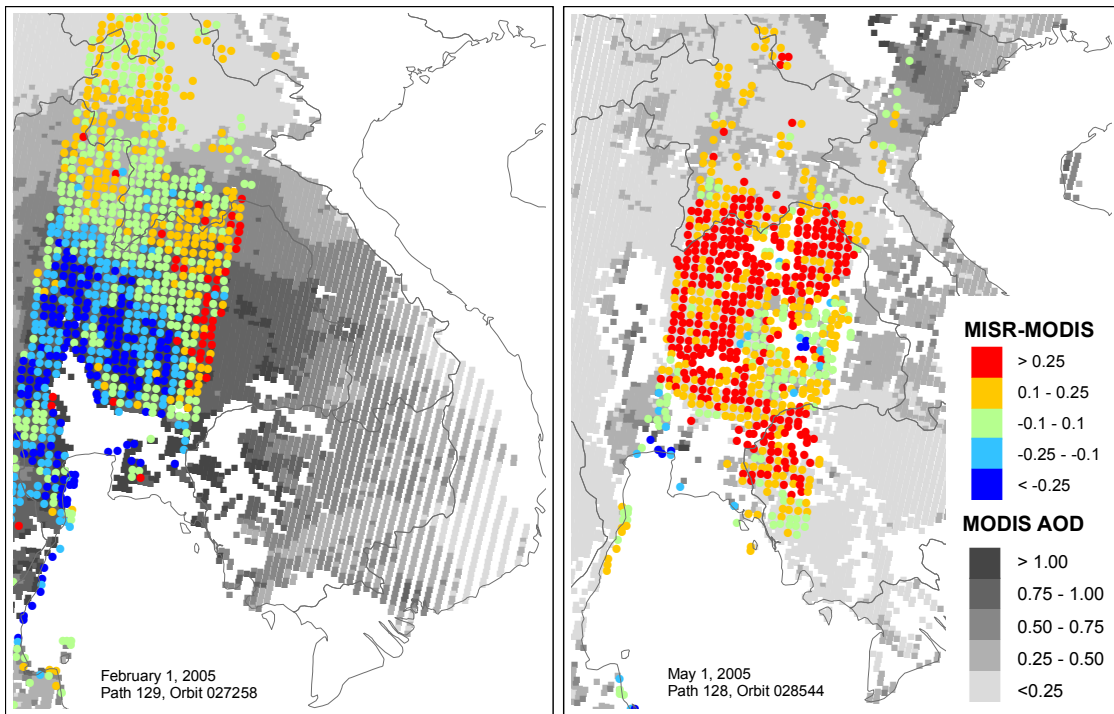


Figure 2: Box plots of the difference between MISR and MODIS AOD retrievals. The three bands are coded in corresponding colors. Dates shown include all 22 days examined in this study.



(A)



(B)

Figure 3: Spatial patterns of the difference between MISR and MODIS AOD retrievals (green band). (A) Five days on MISR path 129, where country outlines are only drawn for the right panel. (B) February 1 and May 1, 2005.

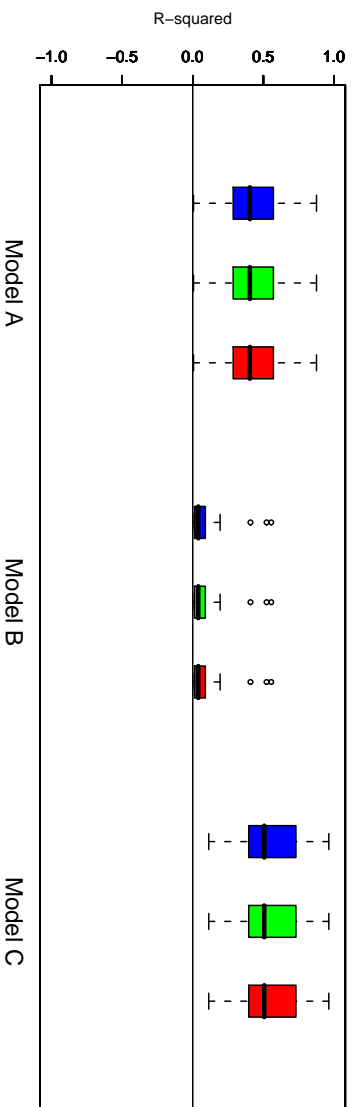
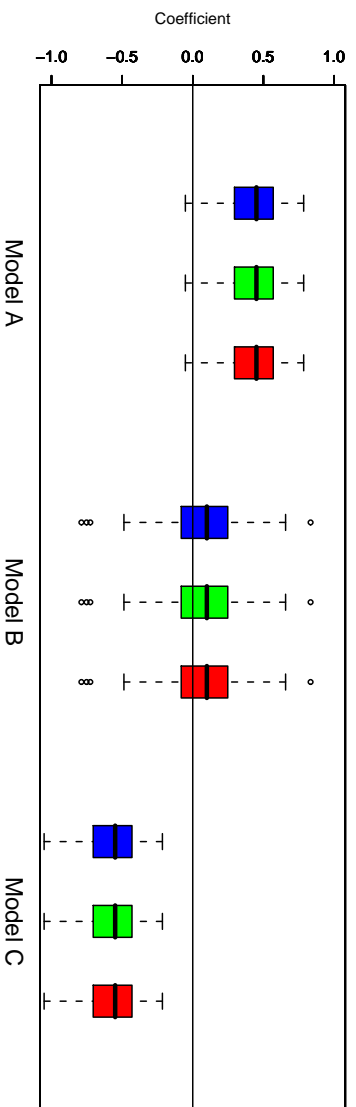
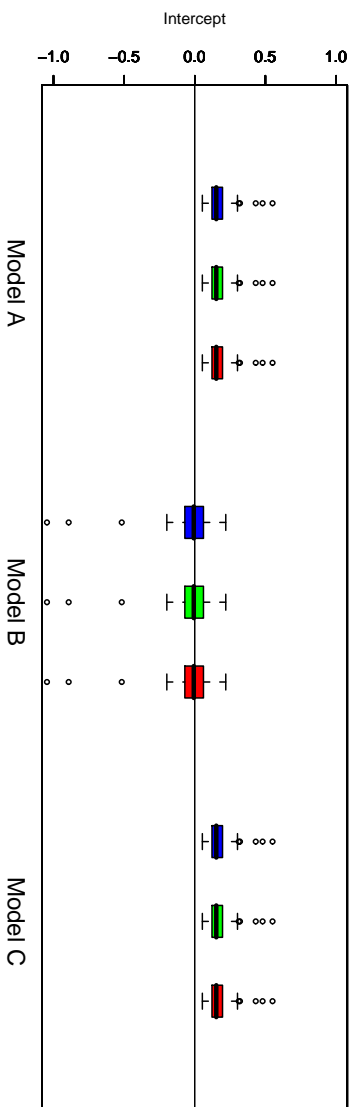


Figure 4: Results of the three regression models. Each box is created using the corresponding estimates obtained from all 22 days used. The three bands are coded in corresponding colors.

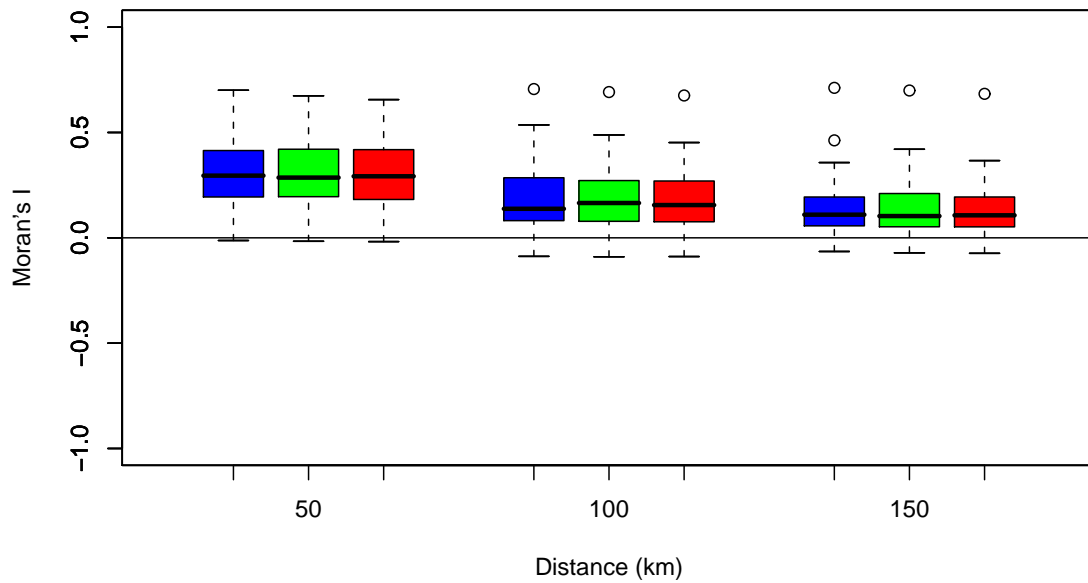


Figure 5: Box plots of the Moran's  $I$  statistic values for three distance thresholds. Each box is created using the Moran's  $I$  values of all available days. The three bands are coded in corresponding colors.

Table 1: Results of the three regression models for all dates simultaneously.

Model	Band	Intercept	Coefficient	$r^2$
Model A	Blue	0.179	0.657	0.741
	Green	0.135	0.632	0.698
	Red	0.112	0.606	0.634
Model B	Blue	0.112	-0.128	0.036
	Green	0.064	-0.105	0.020
	Red	0.028	-0.046	0.003
Model C	Blue	0.179	-0.343	0.438
	Green	0.135	-0.368	0.439
	Red	0.112	-0.394	0.423

Table 2: Results of SAR models.

Covariate	50 km				100 km				150 km			
	Simple model		Extended model		Simple model		Extended model		Simple model		Extended model	
	Estimate	Std. error	Estimate	Std. error	Estimate	Std. error	Estimate	Std. error	Estimate	Std. error	Estimate	Std. error
Intercept	0.227 ***	0.007			0.220 ***	0.014			0.188 ***	0.018		
$\tau^{\text{MOD}}$	-0.776 ***	0.006	-0.780 ***	0.006	-0.762 ***	0.005	-0.776 ***	0.005	-0.725 ***	0.005	-0.741 ***	0.005
dry	0.058 ***	0.008	0.056 ***	0.008	0.072 ***	0.017	0.071 ***	0.017	0.064 **	0.023	0.060 **	0.022
Water			0.233 ***	0.010			0.228 ***	0.017			0.205 ***	0.020
Forest			0.225 ***	0.010			0.213 ***	0.017			0.190 ***	0.020
Shrub			0.245 ***	0.011			0.238 ***	0.017			0.217 ***	0.020
Savanna			0.253 ***	0.010			0.247 ***	0.017			0.228 ***	0.020
Crop			0.250 ***	0.010			0.245 ***	0.017			0.224 ***	0.020
Wetland			0.251 ***	0.028			0.262 ***	0.032			0.250 ***	0.035
Urban			0.219 ***	0.024			0.216 ***	0.028			0.181 ***	0.031
Elevation			0.000 ***	0.000			0.000 ***	0.000			0.000 ***	0.000
droads			-0.030 ***	0.006			-0.033 ***	0.006			-0.029 ***	0.006
dcoast			0.007 ***	0.002			0.000	0.003			0.002	0.002
dbcity			-0.004 **	0.002			0.004 *	0.002			0.001	0.002
docity			0.002	0.005			0.001	0.003			0.001	0.003
$\lambda$	0.893 ***		0.887 ***		0.939 ***		0.939 ***		0.949 ***		0.948 ***	

\* Significant at the 0.01 level.

\*\* Significant at the 0.005 level.

\*\*\* Significant at the 0.001 level.